Newly Identified Forbidden Transitions Within the Ground Configuration of Ions of the Very Low Abundant P, Cl, K, and Co

By

U. Feldman and E. Landi

Artep, Inc. Ellicott City, MD 21042, USA and E.O. Hulburt Center for Space Research,

the Naval Research Laboratory, Washington DC, 20375-5320, USA

and

W. Curdt

Max-Planck-Institut fur Aeronomie, D-37191Katlenburg-Lindau, Germany

February 9, 2003

Submitted for publication to the Astrophysical Journal

Abstract

Forbidden lines resulting from transitions within the ground configuration of highly ionized atoms occupy an important role in diagnosing the properties of astrophysical plasmas. In this paper we report the identification of forbidden lines in the 500-1500 Å range resulting from transitions within the ground configuration of highly ionized ions of the very low abundant phosphorus, chlorine, potassium and cobalt that were recorded by SUMER/SOHO. For the newly identified lines we provide upper level fractional populations multiplied by relevant spontaneous decay rates. Aided by the newly identified lines the coronal composition of elements with photospheric abundances of $5x10^{-7}$-$1x10^{-8}$ relative to hydrogen could be established.

Subject headings: line: identification-Sun: corona-Sun-UV radiation

1. Introduction

Since January 1996 the Solar Ultraviolet Measurements of Emitted Radiation (SUMER) spectrograph on the Solar and Heliospheric Observatory (*SOHO*) is recording high-resolution far-ultraviolet spectra from a variety of regions on and off the solar disk. The majority of bright resonance lines emitted from high-temperature ($T_e \geq 8x10^5$ K) astrophysical plasmas appear at shorter wavelengths than 500 Å, nevertheless the SUMER instrument succeeded in recording a large number of bright resonance and forbidden coronal lines. The intensities and intensity ratios of many of the detected lines can be used to determine plasma properties such as electron densities, electron temperatures, and emission measure distributions. Since the lines in the SUMER spectral range originate from many elements, they are in particular suitable for determining the composition of the solar upper atmosphere under a variety of physical conditions.

During a five-hour period in late June 1996, SUMER recorded coronal spectra at a height of 21,000 km above the west equatorial limb. Since 1996 coincided with the minimum of the 11 years solar cycle and because the time of the observations no unusual activity was present in the vicinity of the west solar limb, the recorded spectra were typical of the quiet corona during solar minimum. The spectra, which contain about 900 lines, were analyzed and published by Feldman et al. (1997). In the 1997 publication about 40% of the reported lines were unidentified. Since the original publication appeared in press dozens of additional lines were identified as high excitation $2s^22p^k3s$ - $2s^22p^k3p$ and $2s^22p^k3p$ -$2s^22p^k3d$ transitions in Si VII and S IX (Kink et al. 1997), Si VIII and S X (Kink et al. 1999), Fe VII (Ekberg & Feldman 2003a) and Fe VIII (Ekberg & Feldman 2003b).

On May 9, SUMER observed an off-limb site above the active region NOAA 8537. At 15:24 UT SUMER began observing in the so-called Reference-Spectrum mode, a standard observing mode in which the instrument scanned with some overlap the entire wavelength range in ~43 Å sections. While the observations were underway a C5.1 flare and an M7.6 flare occurred. Using the spectral recordings Feldman et al. (2000) identified a large number of lines typical of high temperature ($T_e \geq 3x10^6$ K) flaring plasmas. A large fraction of the newly identified lines were found to belong to transitions within ground configurations of the type ns^2np^k where n=2,3 and k=1-5.

As a result of the new identifications, with the exception of iron, practically all degrees of ionization of astrophysically abundant elements with abundance greater than $2x10^{-5}$ that of hydrogen expected to be present in the solar upper atmosphere were identified in the SUMER spectra, e.g., H I; He I-II; C I-IV; N I-V; O I-VI; Ne IV-IX; Mg V-XI; Si II-XIII; S II-XII. Thus far lines from the following iron ions were also identified in the SUMER spectra: Fe II-III, Fe VII-VIII, Fe X-XII, Fe XVII-XXIII. It is expected that lines from several of the missing degrees of ionization will be identified in SUMER spectra once their wavelengths become known. In the case of the moderately abundant elements with abundance $1.5x10^{-6}$ to $3x10^{-6}$ that of hydrogen, lines from a substantial number of ions have been found in the SUMER spectra: e.g., Na V-X; Al VI-XI; Ar IV-IX, Ar XI-XIII; Ca VII-X, Ca XIII-XV; Ni XIII-XV, Ni XX-XXI, Ni XXIII.

The last group of elements that is expected to contribute lines to SUMER spectral range is P, Cl, K, Ti, Cr, Mn, and Co that is substantially less abundant ($1x10^{-8}$ to$5x10^{-7}$ that of hydrogen). Thus far only a small number of lines emitted from these elements were identified in the SUMER spectra and most were identified in the high temperature flare plasma. The identified lines belong to P IV, V, IX, XII; Cl VII; K IX, XII, XIII; Ti XV-XVI; Cr XVI-XVIII, Cr XX; Mn XVII-XIX, Mn XXI; Co XIX. As expected, no line from the extremely low abundant Li, Be, B, Sc or V (less than $1x10^{-8}$ that of hydrogen) has been detected in SUMER spectra.

The intent of this paper is to use a long-exposure spectrum above a quiet coronal region that was acquired in 2000 June and an active region spectrum recorded in 2001 April, to identify lines typical of the quiet and active coronal plasmas ($T_e \leq 3x10^6$ K) belonging to the lowest abundance group of elements mentioned above. Since P and Cl have a first ionization potential (FIP) that is larger than 10 eV they belong to the so-called high-FIP group of elements. K on the other hand has one of the lowest FIP in the periodic table. By identifying lines from these elements we hope to substantially increase the number of high-FIP as well as the very low-FIP lines available for coronal studies of the dependence of the coronal composition on the FIPs.

In Section 2 of the paper we briefly discuss the SUMER instrument and the spectra used in the study. In Section 3 we provide the identifications and wavelengths of the reported lines and in section 4 a short summary of the results is given.

2. The SUMER instrument

The SUMER instrument is composed of a telescope and a spectrometer capable of producing stigmatic high-resolution spectra of any region within a 64x64 arcmin^2 field of view centered on the Sun. The spectrometer consists of the entrance slit off-axis parabolic mirror which collimates the light leaving the slit, a flat mirror which deflects the light onto a concave grating in a Wadsworth configuration, and two imaging detectors. Detector A, used to record the spectra used in the present study, covers the 780 Å-1610 Å range in first order of diffraction. Second order lines are superimposed on the first order spectrum. The SUMER optical surfaces are of silicon carbide, which is a fairly poor reflector for radiation with wavelengths shorter than 500 Å. Details of the SUMER instrument and its modes of operation are described in Wilhelm et al (1995, 1997).

The lines reported in this paper were measured from two different off-limb observations, one from quiet Sun and the other from an active region. The quiet Sun observation was carried out as part of the Joint Observing Program JOP 112 during the week of 2000 June 13-19. A description of the full dataset is given in Parenti et al. (2003). In the present work we have considered only a subset of the JOP 112 SUMER observations. This subset consists of a series of five different observations of the entire SUMER spectral range obtained from a streamer in the southeast limb. The 4”x300” slit used during the observations was always centered at –600”;-941” relative to Sun center, so that the slit imaged the solar corona from 1.05 to 1.30 $R_\odot$. Each of the five spectral scans included the full SUMER wavelength range, divided in 38 windows each ~43 Å wide. Each window was observed with an integration time 300 s, repeated for three consecutive times. We have decompressed and corrected the observations from the flat field and geometrical distortions using the standard SUMER software, for each spectral window. We have first averaged the three consecutive observations, then we averaged the data from the five observations, thus if the nominal exposure time is still 300 s, the signal to noise corresponds to an effective exposure time of 4500 s (75 minutes), providing the highest quality spectrum ever achieved in the corona in the 500-1600 Å range. Since the five observations were taken at different times in the 2000, June 13-19 week, after moving the SUMER slit in the north-south direction, systematic offsets were present from one observation to the other, along the wavelength direction. These were corrected by co-aligning the slit-averaged spectra of the strongest lines in each spectral window. Corrections to these offsets were typically smaller than 2 pixels (80 mÅ). We have averaged the spectra of the 30 pixels corresponding to distances of 1.06-1.10 $R_\odot$.

The active region observation was taken on 2001 April 4 on a large active region at the west limb. The 1”x300” slit center was placed at +954”;+500” relative to Sun center and the 1” wide field of view went from 1.05 to 1.20 $R_\odot$. The exposure time was 300” for each of the 38 sections in which the spectrum was divided. The raw data where decompressed, and corrected for flat field and geometrical distortions using the standard SUMER software. We have selected and averaged the spectra of the 30 pixels closest to the solar limb, where the coronal emission was strongest. Systematic uncertainties in measured wavelengths are between 0.02 and 0.05 Å depending on the quality of the wavelength standards in the vicinity of the measured line.

3. The Newly identified lines

Since the emitting plasma in the quiet region did not show activity during the week long observation and its physical parameters were shown to be constant by Parenti et al.

(2003), it is expected that ions that are 7-12 times ionized formed at $0.5x10^6<T_e<2x10^6$ K will contribute most of the lines to the recorded spectra. Some of the bright P, Cl and K lines if present in the spectra will originate from transitions within the ground configurations of the B-I to F-I isoelectronic sequence ions. Similarly the brightest among the Ti, Cr, Mn and Co lines, if present in the spectra, will most likely originate from transitions within the ground configurations of Al-I to Cl-I isoelectronic sequences ions.

The number of forbidden lines arising from transitions within the ground configuration of C-like to O-like ions are only few and often distributed over a wide wavelength range. To identify such lines with a high degree of certainty one needs to have a fairly good energy level predictions and a fairly good idea on the expected intensities, quantities that depends on atomic rates, emission measure and elemental abundances. Fortunately, for the forbidden transitions discussed in this paper both conditions are met. There are very good semi empirical calculations such as those by Edlén (1983a, 1983b, 1984, 1985), which in recent years were checked quite thoroughly. CHIANTI is a comprehensive atomic database that can provide theoretical line intensities using the emission measure of the region measured by Parenti, et al. (2003) and the expected elemental abundances.

3.1 Lines emitted by P, Cl and K ions:

In a series of papers Edlén (1983a, 1983b, 1984, 1985) described results of a study on the energy levels of low configurations from the B-I to F-I isoelectronic sequences. Using Edlén's calculations we have determined which transitions of the low abundance elements are expected to be present in the SUMER wavelength range.

B-I and F-I isoelectronic sequences: Forbidden lines of P, Cl and K ions resulting from levels within the ground configurations $2s^22p$ and $2s^22p^5$ appear at wavelengths longer than the SUMER 1600 Å upper limit.

C-I isoelectronic sequence: The $2s^22p^2$ configuration produces five forbidden lines that result from the $^3P_0$-$^3P_1$, $^3P_1$-$^3P_2$, $^3P_1$-$^1D_2$, $^3P_2$-$^1D_2$ and $^3P_1$-$^1S_0$ transitions. Lines from the $^3P_0$-$^3P_1$ and $^3P_1$-$^3P_2$ transitions appear at wavelengths longer than 1600 Å. The line from the $^3P_1$-$^1S_0$ transition is predicted to appear for P X at 860.01 Å, for Cl XII at 715.90 Å and for K XIV at 603.52 Å. Unfortunately no line that could be attributed to the predicted wavelengths were found in the spectra. The P X line if present is blended with the S VII 859.93 Å line. The P X and Cl XII lines from the $^3P_2$-$^1D_2$ transition are predicted to appear at wavelengths too long to be visible in the SUMER spectra. However, the K XIV line from the same transition, which is predicted to appear at 1476.91 Å was measured at 1477.09 Å. The line resulting from the $^3P_1$-$^1D_2$ transition in Cl XII is predicted to appear at 1464.4 Å and in K XIV at 1209.2 Å. In the June 2000 spectra a line at 1464.45 Å is present and we identified it as the Cl XII transition.

N-I isoelectronic sequence: The $2s^22p^3$ configuration produces eight transitions; four of them have wavelengths too long to be detected by the SUMER instrument. The four transitions producing lines in the SUMER wavelength range in P IX, Cl XI and K XIII are the $^4S_{3/2}$-$^2P_{3/2}$, $^4S_{3/2}$-$^2P_{1/2}$, $^2S_{3/2}$-$^2D_{5/2}$ and $^4S_{3/2}$-$^2D_{3/2}$. Using the predicted wavelengths all four lines in each of these ions were identified in the SUMER spectra. The four P IX lines were already reported in Feldman et al. (1997) and two of the K XIII lines were reported in Feldman et al. (2000). The remaining 5 out of the 6 lines, the three Cl XI lines

(724.68, 1101.26, 1126.51 Å) and the two K XIII lines (594.91, 622.58 Å) were present in the 2000 June spectra and are identified here for the first time.

O-I isoelectronic sequence: The $2s^22p^4$ ground configuration produces five forbidden lines that belong to the $^3P_2$-$^3P_1$, $^3P_1$-$^3P_0$, $^3P_1$-$^1D_2$, $^3P_2$-$^1D_2$ and $^3P_1$-$^1S_0$ transitions. Only two of the transitions ($^3P_2$-$^1D_2$ and $^3P_1$-$^1S_0$) in P VIII, Cl X and K XII produce lines that are at sufficiently short wavelengths to appear in the SUMER range. According to the predictions the $^3P_1$-$^1S_0$ P VIII line should appear at 951.92 Å, the Cl X line should appear at 804.12 and the K XII line at 694.82 Å. All three lines were present in the spectra. The P VIII line was found to be blended with a S IX line at 951.88 Å. Indeed, Bhatia& Landi (2003) reported the S IX line to be blended with an unidentified line, providing 50% of the measured intensity. The Cl X line was also found to be blended with a much brighter S X line at 804.16 Å and the K XII line at 694.82 Å is most likely blended with the Si IX 694.70 Å.

3.2 Lines emitted by Ti, Cr, Mn and Co ions

Predictions of energy levels within the ground configurations of the Al-I to Cl-I isoelectronic sequences were given in Kaufman and Sugar (1986). Using their predictions we investigated the presence in the 2000 June spectra forbidden Ti, Cr, Mn and Co lines resulting from transitions within the ground configuration of Al-I to Cl-I isoelectronic sequences. All Ti forbidden transitions within the ground configurations of Al-I to Cl-I isoelectronic sequences appear at wavelengths longer than 1600 Å.

Al-I and Cl-I isoelectronic sequences: Forbidden lines of Cr, Mn and Co ions resulting from levels within the configurations $3s^23p$ and $3s^23p^5$ appear at wavelengths longer than the SUMER 1600 Å limit.

Si-I isoelectronic sequence: The $3s^23p^2$ ground configuration produces five forbidden lines that result from the $^3P_0$-$^3P_1$, $^3P_1$-$^3P_2$, $^3P_1$-$^1D_2$, $^3P_2$-$^1D_2$ and $^3P_1$-$^1S_0$ transitions. Among all the transitions only the $^3P_1$-$^1S_0$ produces lines at sufficiently short wavelengths to be present in the SUMER data. The Cr XI line is at 1439.99 Å, the Mn XII line is at 1322.23 and the Co XIV line is at 1123.11 Å. Only the Cr XI and the Mn XII are positively identified in the in the 2000 June spectra. These lines were already detected in Skylab spectra by Sandlin et al. (1977) and Sandlin and Tousey (1979).

P-I isoelectronic sequence: The $3s^23p^3$ ground configuration produces eight transitions and lines from six of them appear at wavelengths too long to be detected by the SUMER instrument. The two transitions producing lines in the proper wavelength range in Cr X, Mn XI and Co XIII are the $^4S_{3/2}$-$^2P_{3/2}$, and the $^4S_{3/2}$-$^2P_{1/2}$. Lines from the two transitions in each of the elements were identified in the SUMER spectra. The Cr X lines at 1489.04 Å and 1564.10 Å and the Mn XI lines at 1359.59 Å and 1450.53 Å were first identified in the Skylab spectra (Feldman and Doschek 1977, Sandlin et al. 1977). The Co XIII 1134.10 Å is identified for the first time in the present work.

S-I isoelectronic sequence: The $3s^23p^4$ ground configuration produces five forbidden lines from the transitions $^3P_2$-$^3P_1$, $^3P_1$-$^3P_0$, $^3P_1$-$^1D_2$, $^3P_2$-$^1D_2$ and $^3P_1$-$^1S_0$. Only the $^3P_1$-$^1S_0$ transition produces lines at sufficiently short wavelengths to be visible in the SUMER spectra. The lines are predicted to be in Mn X at 1574.2 Å and in Co XII at 1368.7 Å. The Co XII line is the only one visible in the recorded spectra.

The newly identified P, Cl, K and Co lines are listed in Table 1. Energy levels of the $2s^22p^3$ ground configuration in Cl^{+10} and K^{+12} derived from the newly identified lines are listed in Table 2. Some of the lines presented in Table 1 were listed as unidentified lines in measurements obtained from the coronal spectra at a height of 21000 km above the quiet limb (Feldman et al. 1997). Intensity ratios between the 1126.51 Å and 1101.26 Å Cl XI lines are sensitive to electron density changes over the two orders of magnitude spanning the $n_e=10^{8.2}$ and $10^{10.2}$ cm^{-3} range (for details see Figure 1).

Table 3 provides for each of the newly identified lines the value $E(T)=n_j^{x+n}/n^{x+m}A_{ji}hc/\lambda_{ij}$ per ion, where n_j^{x+n}/n^{x+m} is fractional populations of its upper level, A_{ji} is spontaneous decay rate from the upper to lower level, and λ_{ij} is the wavelength in Å and $hc=1.98x10^{-8}$ erg Å Temperatures were selected to be on both sides of T_{max}, where T_{max} is the temperature of maximum fractional ion abundance (Mazzotta et al. 1988). The atomic data used to calculate E(T) for P VIII, K XII, K XIII and K XIV are based on rate calculation stored in CHIANTI (Dere et al 1997, Young et al 2003). The atomic data for Cl X, Cl XI, Cl XII are based on interpolated rates from CHIANTI while those for Co XII, Co XIII are based on extrapolations. It is expected that the extrapolated rates are least accurate.

4. Summary

In this work we report the new identification of one P line, five Cl lines, three K lines and two Co lines. Four additional P forbidden lines and four K forbidden lines also observed here were identified in the earlier SUMER studies.

The forbidden lines expected from transitions within the ground configurations of the Ti ions that belong to the Al-I to Cl I isoelectronic sequences appear at wavelengths that are too long to be detectable by SUMER. For Cr three lines and for both Mn and Co four lines belonging to the Al-I to Cl-I isoelectronic sequences are in the SUMER range. Although the three Cr and three of the Mn lines were first identified in Skylab spectra the Co lines were identified for the first time in the SUMER 2000 June spectra. An account of the P, Cl, K forbidden lines belonging to transitions within ground configurations of the type $2s^22p^k$ expected to be present in the SUMER range and those that were identified are given in Tables 4-6. Similarly an account of the Cr, Mn and Co forbidden lines belonging to transitions within the ground configurations of the type $3s^23p^k$ expected to be present in the SUMER range and those that were identified are given in Tables 7-9.

With the exception of S and Ar all abundant or moderately abundant elements with Z>10 have a low first ionization potential (low-FIP). By identifying in the SUMER spectra lines from P (I.P=10.49 eV), and Cl (I.P.=12.97 eV), the number of lines from elements with high-FIP (I.P.>10 eV) increases significantly. Using the newly identified lines the probability of finding lines from high- and low-FIP ions that possess similar temperature dependencies increases. It is of value of remember that K is one of lowest FIP elements (I.P.=4.34 eV) found in the periodic table. As a result of this and earlier studies of spectra emitted by coronal plasmas ($T_e \geq 3x10^6$ K) 24 out of the 34 possible forbidden lines belonging to P, Cl, K, Cr, Mn and Co in the 500-1600Å range are present in SUMER spectra.

In Figure 2 we displays ion fractions taken from Mazzotta et al. (1998) for some of the newly identified minor elements (full curves) together with more abundant elements (dashed curves). The upper left panel displays the ion fractions of Co^{+11} and Co^{+12} (full lines) vs. the Fe^{+11} and Fe^{+12} (dashed lines), two low FIP elements. The upper right panel displays the ion fractions of the very low-FIP K^{+11}, K^{+12} and K^{+13} (full lines) vs. the high-FIP Ar^{+10}, Ar^{+11} and Ar^{+12} (dashed curves). The lower left panel displays the ion fractions of the high-FIP Cl^{+9}, Cl^{+10} and Cl^{+11} (full lines) vs. the low-FIP Fe^{+11}, Fe^{+12} and Fe^{+16} (dashed curves). The lower right panel displays the ion fractions of the high-FIP P^{+7} (full lines) vs. the low-FIP Si^{+7} (dashed curves).

Acknowledgments: The SUMER project is financially supported by DLR, CNES, NASA and the ESA PRODEX Program (Swiss contribution). SUMER is part of SOHO, the Solar and Heliospheric Observatory, of ESA and NASA. The work of UF and EL was supported by the ONR and by NASA SR&T Grant.

References

Bhatia, A.K. & Landi, E. 2003 ADNDT, n press

Dere, K.P., Landi, E., Mason, H.E., Monsignori Fossi, B.C., & Young, P.R. 1997, A&AS, 125, 149

Edlén, B. 1983a, Physica Scripta, 28, 51

Edlén, B. 1983b, Physica Scripta, 28, 483

Edlén, B. 1984, Physica Scripta, 30, 135

Edlén, B. 1985, Physica Scripta, 31, 345

Ekberg, J & Feldman, U. 2003a ApJ 595, Sept 20 issue

Ekberg, J & Feldman, U. 2003b ApJS 148, Oct. issue

Feldman, U., & Doschek, G.A. J. Opt. Soc. Am. 67, 726

Feldman, U., Behring, W.E., Curdt, W., Schühle, U., Wilhelm, K., Lemaire, P., & Moran, T.M. 1997, *ApJ Suppl.,* 113, 195

Feldman, U., Curdt, W., Landi, E. & Wilhelm, K. 2000, *ApJ* 544, 508

Kaufman, V,. & Sugar, J. 1986, J. Phys. Chem. Ref. Data, 15, 321

Kink, I., Jupén, C., Engström, L., Feldman, U., Laming M., & Schühle, U. 1997, ApJ, 487, 956.

Kink, L., Engström, L. & Feldman, U. 1999, ApJ*,* 512, 496.

Mazzotta, P., Mazittelli, G., Colafrancesco, S., & Vittorio, N 1998, A&AS 133, 403

Parenti, S., Landi, E., & Bromage, B.J.I. 2003, ApJ, 590, 519

Sandlin, G.D., Brueckner, G.E., & Tousey, R. 1977, ApJ, 227, L107

Sandlin, G.D., & Tousey, R. 1979, ApJ, 214, 898

Wilhelm, K. et al. 1995, Solar Phys., 162, 189

Wilhelm, K. et al. 1997, Solar Phys., 170, 75

Young, P.R., Del Zanna, G., Landi, E., Dere, K.P., Mason, H.E., & Landini, M. 2003, ApJS, 144, 13

Table 1 Newly identified forbidden transitions within the ground configuration of P, Cl, K and Co ions

Ion	λ Å[1] Measured	λ Å Predicted	Transition	Comments
K XIII	594.91	594.94[2]	$2s^22p^3\ ^4S_{3/2}$-$^2P_{3/2}$	Blended[6] with 1st order Mg VII line (1189.84 Å)
K XIII	622.58[3]	622.51[2]	$2s^22p^3\ ^4S_{3/2}$-$^2P_{1/2}$	
K XII	694.82	694.82[4]	$2s^22p^4\ ^3P_1$-$^1S_0$	
Cl XI	724.68	724.76[2]	$2s^22p^3\ ^4S_{3/2}$-$^2P_{1/2}$	
Cl X	804.16[3] bl	804.12[4]	$2s^22p^4\ ^3P_1$-$^1S_0$	Blended[6] with S X
P VIII	951.88 bl	951.92[4]	$2s^22p^4\ ^3P_1$-$^1S_0$	Blended[6] with a S IX line
Cl XI	1101.26[3]	1101.24[2]	$2s^22p^3\ ^4S_{3/2}$-$^2D_{5/2}$	
Cl XI	1126.51	1126.54[2]	$2s^22p^3\ ^4S_{3/2}$-$^2D_{3/2}$	
Co XIII	1134.10	1134.17[5]	$3s^23p^3\ ^4S_{3/2}$-$^2P_{3/2}$	
Co XII	1368.78	1368.7[5]	$3s^23p^4\ ^3P_1$-$^1S_0$	
Cl XII	1464.45[3]	1464.28[4]	$2s^22p^2\ ^3P_1$-$^1D_2$	
K XIV	1477.19	1476.91[4]	$2s^22p^2\ ^3P_2$-$^1D_2$	

[1] Wavelengths of λ< 800 Å were measured in second order.
[2] Predictions from Edlén (1984)
[3] Unidentified line in Feldman et al. (1997)
[4] Predictions from Edlén (1985)
[5] Predictions from Kaufman & Sugar (1986)
[6] Blended, unresolved

Table 2. Energy levels in the $2s^22p^3$ ground configuration of Cl and K

Level	Cl^{+10}	K^{+12}
	Energy (cm^{-1})	Energy (cm^{-1})
$^4S_{3/2}$	0	0
$^2D_{3/2}$	88770±2	100559[1]±4
$^2D_{5/2}$	90805±2	105722[1]±4
$^2P_{1/2}$	137992±4	160622±4
$^2P_{3/2}$		168093±4

[1]Original wavelength measurements were reported by Feldman et al. (2000)

Table 3 Upper level fractional population multiplied by the spontaneous decay between upper and lower levels at densities of $1x10^{8}$ cm^{-3} and temperatures where the ion fractional abundances are expected to be significant

Ion	λ (Å)	E[1] (10^{-14} erg s^{-1}) vs. Log (T_e)											
		5.7	5.8	5.9	6.0	6.1	6.2	6.3	6.4	6.5	6.6	6.7	6.8
P VIII	951.88	18.9	17.9	16.9	15.7	14.4	13.2	12.0	10.9				
Cl X	804.16	9.51	8.95	8.24	7.44	6.59	5.74	4.93	4.19	3.52			
Cl XI	724.68			10.1	9.18	8.16	7.12	6.12	5.19	4.34	3.58		
Cl XI	1101.26			37.0	33.5	29.9	26.3	22.9	19.7	16.7	14.0		
Cl XI	1126.51			42.4	38.2	33.8	29.5	25.4	21.6	18.1	15.1		
Cl XII	1464.45				8.64	7.68	6.73	5.82	4.98	4.21	3.53	2.93	2.41
K XII	694.82			7.05	6.50	5.88	5.22	4.56	3.93	3.35	2.84	2.38	
K XIII	594.91					14.1	12.6	11.1	9.68	8.30	7.04	5.91	4.91
K XIII	622.58					8.06	7.17	6.27	5.40	4.59	3.85	3.20	2.64
K XIV	1477.19						9.25	8.15	7.10	6.11	5.20	4.39	3.68
Co XII	1368.78		2.51	2.27	2.03	1.80	1.58	1.37	1.19	1.03			
Co XIII	1134.10			1.18	1.61	1.41	1.23	1.07	0.92	0.79	0.68		

[1] Atomic data for P VIII, K XII, XIII, XIV are from CHIANTI (Dere et al 1997, Young et al 2003). The atomic data for the rest of the lines in the table are from interpolations of rates from adjacent ions along the isoelectronic sequence stored in the CHIANTI database.

Table 4. SUMER range forbidden transitions within the $2s^22p^2$ ground configuration of the C I isoelectronic sequence

Ion	T_e (K)	$^3P_0$-$^3P_1$	$^3P_1$-$^1D_2$	$^3P_2$-$^1D_2$	$^3P_1$-$^1S_0$
		λ (Å)	λ (Å)	λ (Å)	λ[1] (Å)
P X	1.4×10^6				[860.01[1]]
Cl XII	2.3×10^6		1464.45		[715.90[1]]
K XIV	3.2×10^6		[1209.25[1]]	1477.19	[603.45[1]]

[1]Wavelengths in square parentheses are from Edlén (1985)

Table 5. SUMER range forbidden transitions within the $2s^22p^3$ ground configuration of the N I isoelectronic sequence

Ion	T_e (K)	$^4S_{3/2}$-$^2P_{3/2}$	$^4S_{3/2}$-$^2P_{1/2}$	$^4S_{3/2}$-$^2D_{5/2}$	$^4S_{3/2}$-$^2D_{3/2}$
		λ (Å)	λ (Å)	λ (Å)	λ (Å)
P IX	1.1×10^6	853.54	861.10	1307.57	1317.66
Cl XI	1.8×10^6	[709.03][1]	724.68	1101.26	1126.51
K XIII	2.8×10^6	594.91	622.58	945.88	994.44

[1]Wavelengths in square parentheses are from Edlén (1984)

Table 6. SUMER range forbidden transitions within the $2s^22p^4$ ground configuration of the O I isoelectronic sequence

Ion	T_e (K)	$^3P_2$-$^1D_2$	$^3P_1$-$^1S_0$
		λ[1] (Å)	λ (Å)
P VIII	7.9×10^5		951.88bl
Cl X	1.3×10^6	[1543.64[1]]	804.16bl
K XII	2.0×10^6	1256.48	694.82bl

[1] Wavelengths in square parentheses are from Edlén (1983a)

Table 7. SUMER range forbidden transitions within the $3s^22p^2$ ground configuration of the Si I isoelectronic sequence

Ion	T_e (K)	$^3P_1$-$^1S_0$
		λ (Å)
Cr XI	1.1×10^6	1439.99
Mn XII	1.4×10^6	1322.23
Co XIV	1.9×10^6	[1123.0[1]]

[1]Wavelengths in square parentheses are from Kaufman & Sugar (1986)

Table 8. SUMER range forbidden transitions within the $3s^23p^3$ ground configuration of the P I isoelectronic sequence

Ion	T_e (K)	$^4S_{3/2}$-$^2P_{3/2}$	$^4S_{3/2}$-$^2P_{1/2}$
		λ (Å)	λ (Å)
Cr X	1.0×10^6	1489.04	1564.10
Mn XI	1.2×10^6	1359.59[1]	1450.53
Co XIII	1.7×10^6	1134.10	[1258.5[1]]

[1]Wavelengths in square parentheses are from Kaufman & Sugar (1986)

Table 9. SUMER range forbidden transitions within the $3s^23p^4$ ground configuration of the S I isoelectronic sequence

Ion	T_e (K)	$^3P_1$-$^1S_0$
		λ (Å)
Mn X	1.0×10^6	[1574.2[1]]
Co XII	1.6×10^6	1368.78

[1]Wavelengths in square parentheses are from Kaufman & Sugar (1986)

Figure captions

1. Intensity ratios of the 1126.54 Å and 1101.24 Å Cl XI lines as a function of electron density

2. A displays ion fractions taken from Mazzotta et al. (1998) for some of the newly identified minor elements (full curves) together with those of more abundant elements (dashed curves). The upper left panel displays the ion fractions of Co^{+11} and Co^{+12} (full lines) vs. the Fe^{+11} and Fe^{+12} (dashed lines), two low FIP elements. The upper right panel displays the ion fractions of the very low-FIP K^{+11}, K^{+12} and K^{+13} (full lines) vs. the high-FIP Ar^{+10}, Ar^{+11} and Ar^{+12} (dashed curves). The lower left panel displays the ion fractions of the high-FIP Cl^{+9}, Cl^{+10} and Cl^{+11} (full lines) vs. the low-FIP Fe^{+11}, Fe^{+12} and Fe^{+16} (dashed curves). The lower right panel displays the ion fractions of the high-FIP P^{+7} (full lines) vs. the low-FIP Si^{+7} (dashed curves).

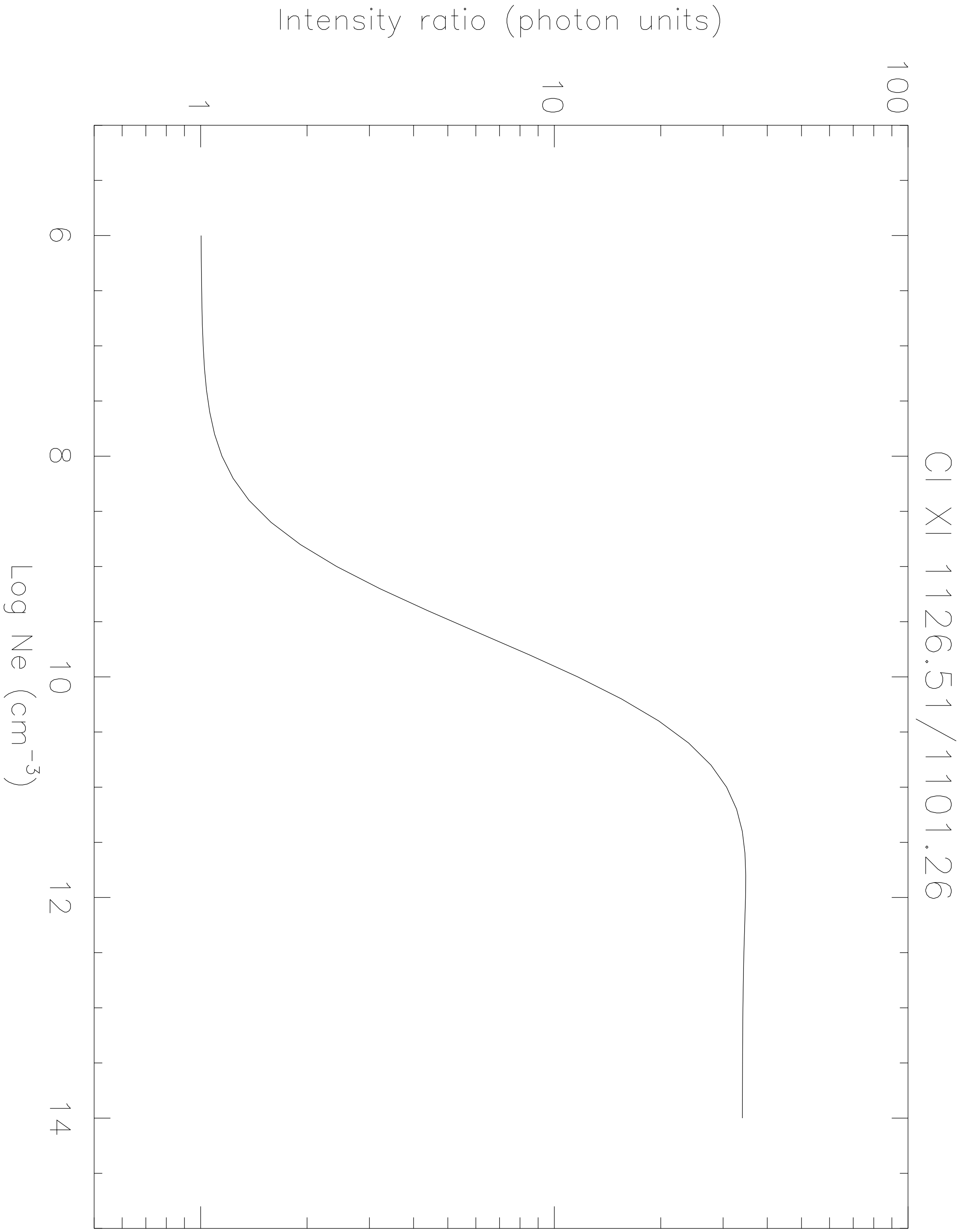
Intensity ratio (photon units)
1
10
100
6
8
10
12
14
Log Ne (cm^{-3})
Cl XI 1126.51/1101.26

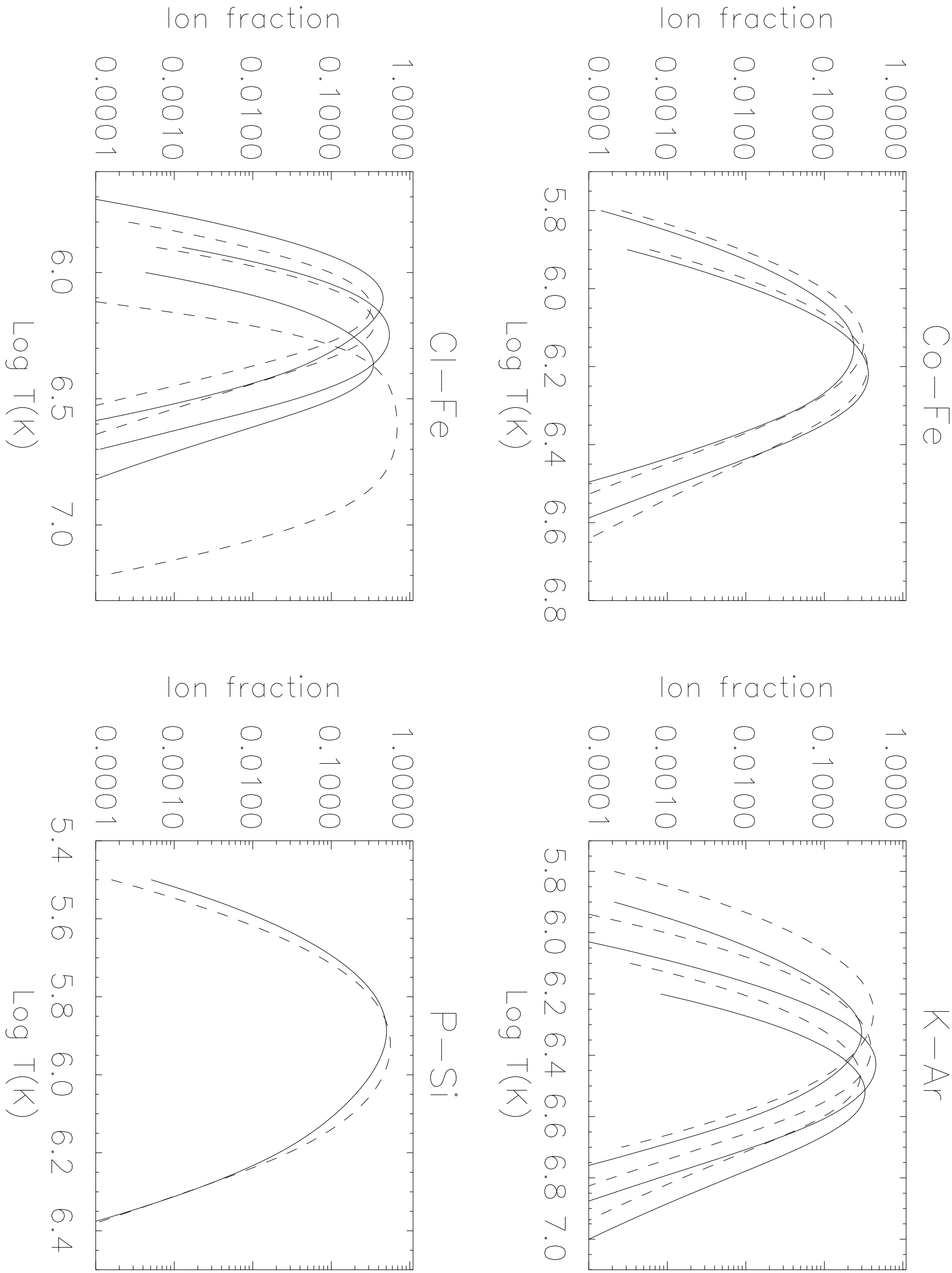
Co—Fe
Ion fraction
1.0000
0.1000
0.0100
0.0010
0.0001
Log T(K)
5.8
6.0
6.2
6.4
6.6
6.8
Cl—Fe
Ion fraction
Log T(K)
6.0
6.5
7.0
K—Ar
Ion fraction
Log T(K)
5.8 6.0 6.2 6.4 6.6 6.8 7.0
P—Si
Ion fraction
Log T(K)
5.4 5.6 5.8 6.0 6.2 6.4